



Solid phase-fabrication of multi-walled carbon nanotubes and their derivatives for efficient extraction and analysis of Bismarck Brown-Y Dye from aqueous solution

Salah Mahdi Saleh^a, Ali Abdulrazzaq Abdulwahid^{a,*} and Zaki N. Kadhim^a

^a Department of Chemistry, College of Science, University of Basra, Postal Code 61004, Basra, Iraq

ARTICLE INFO:

Received 14 Oct 2023

Revised form 22 Dec 2023

Accepted 5 Feb 2024

Available online 29 March 2024

Keywords:

Solid phase extraction,
 Multi-walled carbon nanotubes,
 UV-Vis spectrophotometer,
 Bismarck Brown-y

ABSTRACT

This investigation used efficient multi-walled carbon nanotubes (MWCNTs) and their derivatives; MWCNT-Tris, MWCNT-H, MWCNT-Tetra and MWCNT-G, for extraction and removing the Bismarck Brown-Y (BB-Y) by solid phase extraction (SPE). The concentration of BB-Y was measured by UV-Vis spectrophotometer after the SPE technique. The solid phases were analyzed and characterized by utilizing several techniques, including Fourier Transform Infrared Spectroscopy (FTIR), Field Emission Scanning Electron Microscopy (FESE), zeta potential measurement, and X-ray Diffraction (XRD). At optimization conditions, the optimum concentration of the BB-y was obtained at 200 mgL⁻¹ and 300 mg L⁻¹ for MWCNT and MWCNT-Tris, whereas 400 mg L⁻¹ for MWCNT-H, MWCNT-Tetra, and MWCNT-G. Additionally, the optimal pH value was 6.0 for MWCNT-Tris, and it was 10 for MWCNT, MWCNT-H, MWCNT-Tetra, and MWCNT-G. However, the volume of samples was achieved at 25 mL. Furthermore, it was found that the most effective flow rate for the eluting solvent was 0.5 ml min⁻¹. Besides the type and volume of eluents were examined and evaluated. Finally, the present work involved the determination of adsorption capacity using Langmuir and Freundlich isotherm models under ideal conditions. The Langmuir model revealed that the q_{max} for the MWCNT, MWCNT-tris, MWCNT-H, MWCNT-Tetra, and MWCNT-G was obtained 862.07, 1075.27, 1282.05, 1298.70, and 1333.33 mg g⁻¹, respectively.

1. Introduction

A living ecosystem requires water as a fundamental element. Although the water covers 1.386 billion square kilometers of the world, approximately 97 percent is made up of salt-water-containing seas and oceans, and over two percent is in the form of ice caps and glaciers. Still, approximately one percent is distributed as rivers, lakes, underground water, and water vapor can be drinking water [1]. Nowadays, one of the most critical problems in the world today

is water contamination by numerous hazardous substances. Multiple harmful pollutants are released into the environment due to the rapid rise of human activities such as industrialization, unplanned urbanization, and careless use of water resources from nature, as well as enormous population growth [2]. Polluted waters include a variety of contaminants, including both inorganic and organic, which include dyes, pesticides, pharmaceuticals, degraded organic waste, and organic pollution. Besides, harmful heavy elements represent inorganic pollutants [3]. The dyes are colored organic materials used in various industries including clothing, textiles, leather, plastic, paper, medicine, beauty products, and food. They also color hair, fur, petroleum products, and lubricants.

*Corresponding Author: Ali A. Abdulwahid

Email: ali.abdulwahid@uobasrah.edu.iq

<https://doi.org/10.24200/amecj.v7.i01.307>

Moreover, dyes represent one of the pollutants with the most hazardous chemicals of all those productions. According to the report, around 200,000 tons of dyes are utilized in industries annually, and their chromophore-containing chemical effluent is improperly treated before being drained into water [4]. The effect of dyes and other pollutants starts when discharged into the environment, particularly those that are harmful to living creatures [5]. Typically, dyestuffs offer outstanding coverage when used at relatively low concentrations as a result of their high intensity of color which lead to unwilling color changes in the waste brought on by the dyes and can prevent sunlight from penetrating due to the effect on consumption of dissolved oxygen, hence inhibiting photosynthesis process. Besides, the colored textile effluent also makes the water more mutagenic, carcinogenic, and gene-toxic, all of which pose serious risks to the environment as well as flora and fauna [6-8]. In 1856, Perkin produced the first manufactured dye, mauveine, an aniline dye [9]. Natural and artificial dyes are the two main groups that are based on the raw ingredients used. Natural dyes are produced by using trees, plants, and other elements of nature. However, synthetic dyes, are produced by using chemicals and oil [10]. There is another classification of dyes depending on either their structure or their application, based on their structural characteristics, the following dyes are categorized: azo, nitro, phthalein, triphenyl methane, indigo, and anthraquinone while, the classification of dyes based on their application, including acid dye, basic dye, direct dye, ingrain dye, dispersed dye, mild dye, vat dye, and reactive dyes [11]. Nevertheless, due to their intricate chemical compositions, dyes are very impervious to decay. Consequently, they often remain stable in a variety of circumstances, including aerobic digestion, heat, light, and oxidizing factors [12]. Therefore, different ways to remove dyestuffs from wastewater before discharging into the environment are membrane filtration, coagulation, flocculation, adsorption, modified oxidation processes, photocatalytic degradation, and biological therapy which beyond one of three basic techniques which are physical, biological and chemical [13,14]. Traditional physical techniques, such as adsorption and separating membranes. The adsorption method is attractive for the removal of colors even though dyes are resistant to oxidation, and biodegradation, as well as being stable to light and heat. Furthermore, the adsorption method is effective and doesn't need any further preprocessing before being used. Besides, it is regarded cheap and optimal method [15,16]. Solid phase extraction (SPE) is a conventional approach to acquire adequate samples for analysis. The partition coefficient between the mobile/aqueous

phase and the adsorbent is what determines how the analyte is separated. There have been reports of various modified SPEs. The most popular types of SPE include column SPE, pipette tip SPE (PT-SPE), magnetic solid phase extraction (MSPE), and dispersive solid phase extraction (DSPE) [17]. SPE for preconditioning samples has several benefits, including quick separation, low prices, little solvent use, high enrichment efficiency and recovery rate, rapid processing times, no emulsion creation, and the flexibility to be used with various analytical detection techniques [18]. As adsorbent materials carbon nanoparticles (CNs) represented by graphene, graphene oxide, carbon nano-disks, carbon nanotube rings, either single or multiwall, and carbon nanocones, are commonly employed in SPE [19]. As opposed to typical adsorbent materials, CNTs offer great chemical stability, higher surface area, smaller pore size, hollow structure, and ease of modifying; these benefits make CNTs a more favorable adsorbent than traditional adsorbent for preparing samples techniques in addition to their purity, surface area, functional groups on the surface, adsorption sites, and experimental settings, CNTs' adsorption effectiveness also depends on these factors [20]. Also, dyes and other organic compounds (BTEX) can be extracted by nanostructures such as CNTs, graphene (G), graphene oxide(GO), silica (SiO₂), and Metal-organic frameworks (MOFs) by SPE methods before being determined by the liquid or gas chromatography (GC-FID/ GC-MS/ HPLC) in liquid phases [21-27]. This paper aims to examine the feasibility of utilizing a multi-walled carbon nanotube and its derivatives as a solid phase in solid-phase extraction (SPE) for the purification of water contaminated with organic hazardous dye Bismarck Brown-y, 1,3-Benzenediamine, 4,40 -[1,3-phenylenebis (2,1-diazenediyl)] bis-, hydrochloride (1:2) (Fig.1).

2. Experimental

2.1. Chemicals and Materials

Bismarck-Brown Y has been purchased from Merck Company with molecular formula and weight of C₁₈H₂₀Cl₂N₈ and Mw 419.31 g mol⁻¹, respectively (CAS Number: 10114-58-6). In addition, graphite fine powder and DCC (N, N'- Dicyclohexylcarbodiimide, CAS Number: 538-75-0) were from Merck company. Stock solutions from all dyes was prepared by dissolving (1000 mg L⁻¹) in distilled water. PH was adjusted by 0.1- 0.01 mol L⁻¹ from two solutions NaOH (CAS Number:1310-73-2, Merck) and HCl (GCC). Potassium chlorate was purchased from Sigma-Aldrich. According to each manufacturing company, the liquid solvents have been listed as follows: pure ethanol (J.T. Baker), pure methanol (Himedia),

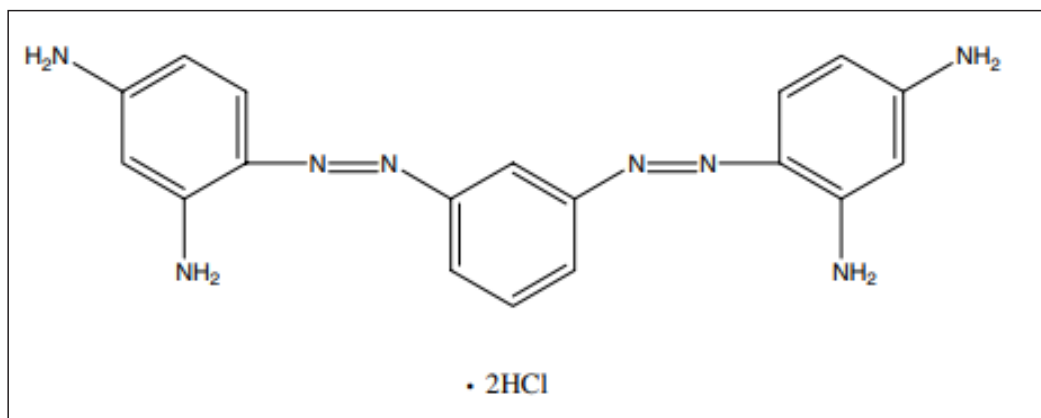


Fig. 1. Chemical Structure of Bismarck Brown-Y

dimethylsulfoxide (Himedia), dimethylformamide (GCC), nitric acid (GCC) and sulfuric acid (J.T. Baker). The identification of multi-walled carbon nanotubes (MWCNTs) and their derivatives was achieved through the utilization of various analytical techniques, including Fourier-transform infrared spectroscopy (FT-IR), X-ray diffraction (XRD), transmission electron microscopy (TEM), and scanning electron microscopy (SEM). The absorbance measurement for the BB-Y dye solution was conducted at a specific wavelength of 455.5 nm, utilizing a UV-visible spectrophotometer (PG Instrument T80 + UV-Vis). The dye removal efficiency (R%) is expressed as a percentage and the quantity of BB-y dye absorbed per unit weight of absorbent at a given time. Also, q (mg g^{-1}) was determined using Equation 1.

$$q_e = (C_0 - C_e) \times V/m \quad (\text{Eq.1})$$

C_e referred to the concentration of Bismarck Brown-y in (mg L^{-1}) at time t , whereas C_0 pointed out the initial concentration in (mg L^{-1}) of the same dye. However,

V represents the volume of dye in a (L), while m is the weight of the solid phase in (g).

2.2. Preparation of Multi-Walled Carbon Nanotube

The modified Staudenmaier approach was used in this investigation to create MWCNTs. The graphite powder was added based on stirring to the mixture which consisted of concentration of H_2SO_4 and HNO_3 in (1.0 g: 10v: 5v) ratio (mass: volume: volume) for 30 min, then cooling the solution at 5C^0 in the ice bath with forcefully stirring. KClO_3 with ratio to graphite (5: 1) (mass: mass) was slowly added to the solution and gradually increased the heat until 75C^0 and stayed overnight. After that, the solution was left in dry air for three days. Most of the graphite precipitated on the bottom. However, some reacting carbons were floating. One liter of DI water was added to the floating carbon particles after collecting them with one hour of vigorous stirring, and then the solution was rapidly filtered and dried [28].

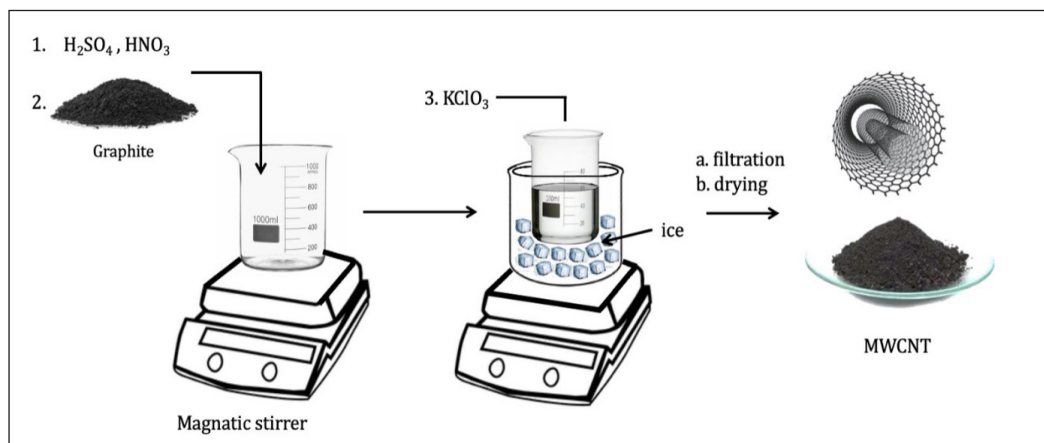


Fig. 2. Step of preparation of multi-walled carbon nanotube

2.3. Purification of MWCNTs

A 0.05 g of impure MWCNTs was heated at 350 C° for two hours to eliminate amorphous carbon and catalyst impurities. After being cooled to room temperature for more emphasis to eliminate additional impurities, the heat-treated MWCNTs were ultrasonically for 4 hours in 20 mL of concentrated HCl then repeatedly rinsed with water until the pH became neutral, and then dried at 100 C° in an air oven.

2.4. Functionalization of MWCNTs

Nitric acid and sulfuric acid were mixed to perform chemical oxidation, where 0.1 g of pristine MWCNTs was added to a mixture consisting of 4.0 M and 10.0 M, respectively, with an ultimate volume of 20 mL in the ratio (1:3) to reduce the damage of the nanotubes. The mixture was stirred magnetically at room temperature for 18 hours.

2.5. Modification of MWCNT-COOH with Amino compound

Carboxyl groups, which allotrope in the structure of MWCNTs, interacted with amine groups to form a new group known as an amide group. Consequently, 1.0 g of MWCNT-COOH was taken and placed in a beaker (100 mL), then 1.0 g of DCC was poured into the beaker after being dissolved in 20 mL of DMF solvent. The mixtures were left at room temperature with constant stirring for 30 minutes. In the following step, 60 mL of methanolic solution was added to the mixture above, which already contained 1.0 g of either 4, 4'-Methylenedianiline, tris-(hydroxymethyl) aminomethane and tetraethylenepentamine or 2, 6-diamine pyridine. The solution is kept at 60 C° for 24

hours with continuous stirring. The resultant mixture was centrifuged at 2500 rpm to separate it. After multiple washes with DMF-Methanol solution and DW, the black precipitate was produced after drying it for 10 hours at 70°C [29].

2.6. Solid Phase Extraction

Three basic steps were applied in the solid phase extraction (SPE) technique: column preparation step, loading step, and elution step [30]. The polypropylene tube (injection tube) was utilized in this study as a column (cartridge), as shown in Figure 3. The column was packed with a one mm thickness of permeable film from polypropylene (disc), followed by four layers of glass filter paper sheets. Subsequently, the column was loaded with an amount weight of the prepared solid phase, in this study, which was either MWCNT, MWCNT/G, MWCNT/Tris, MWCNT/Tetra, or MWCNT/H. The surface of the packed solid phase should be homogeneous and plane with equal height. Moreover, as a last step in the column preparation, 10 ml of ionic water was passed through the column to activate the phase and remove air space. Whereas, in the second step (loading step), the dye solution under the study with neutral pH_{pzc} was passed through the packed solid phase, where the dye will attach with the solid phase in the column, while the unbounding part of the dye and the rest of matrix will pass through the column with flow rate depends on gravity. Finally, and as the last step (elution step), which involved passing the elution solution through the column to rid out the dye from the packed solid phase, the solution was collected to determine the concentration of dye by UV-visible instrument.

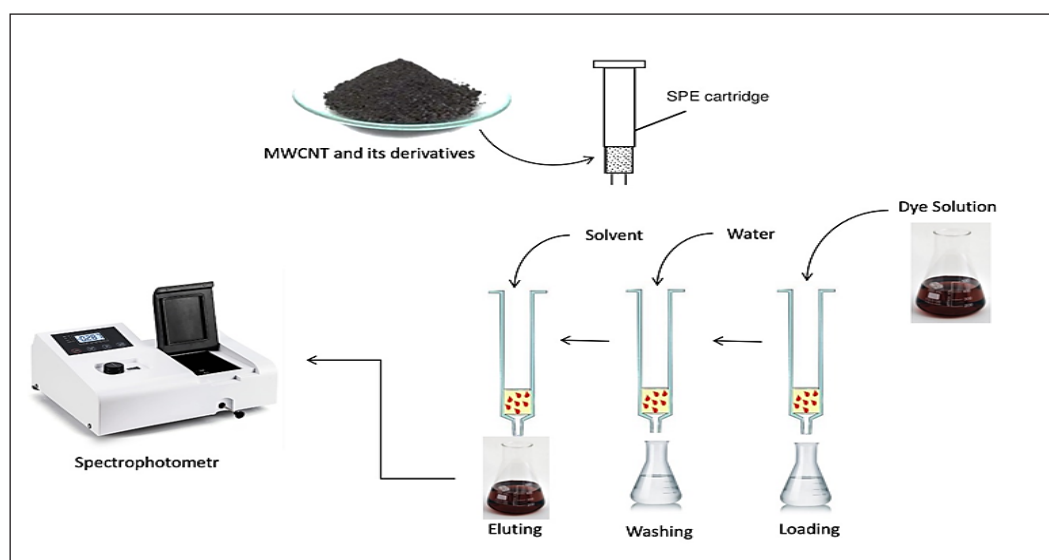


Fig.3. General procedure based on solid phase extraction by MWCNTs, MWCNTs/G, MWCNTs/Tris, MWCNTs/Tetra

2.7. Characterization Methods

To evaluate the surface properties of multi-walled carbon nanotubes (MWCNTs) and their derivatives (MWCNT/G, MWCNT/Tris, MWCNT/Tetra, or MWCNT/H), various analytical techniques, including Fourier-transform infrared spectroscopy (FTIR), X-ray diffraction (XRD, Fig. 4a-e), scanning electron microscopy for MWCNT and their derivatives

(SEM, Fig. 5a-d), and zeta potential were employed for analysis. Fourier Transform Infrared (FT-IR) spectroscopy was employed to ascertain the sort and characteristics of the functional groups present in the synthesized solid phases (Tables 1 and 2). Including these functional categories enhances diversity and, consequently, the extraction process.

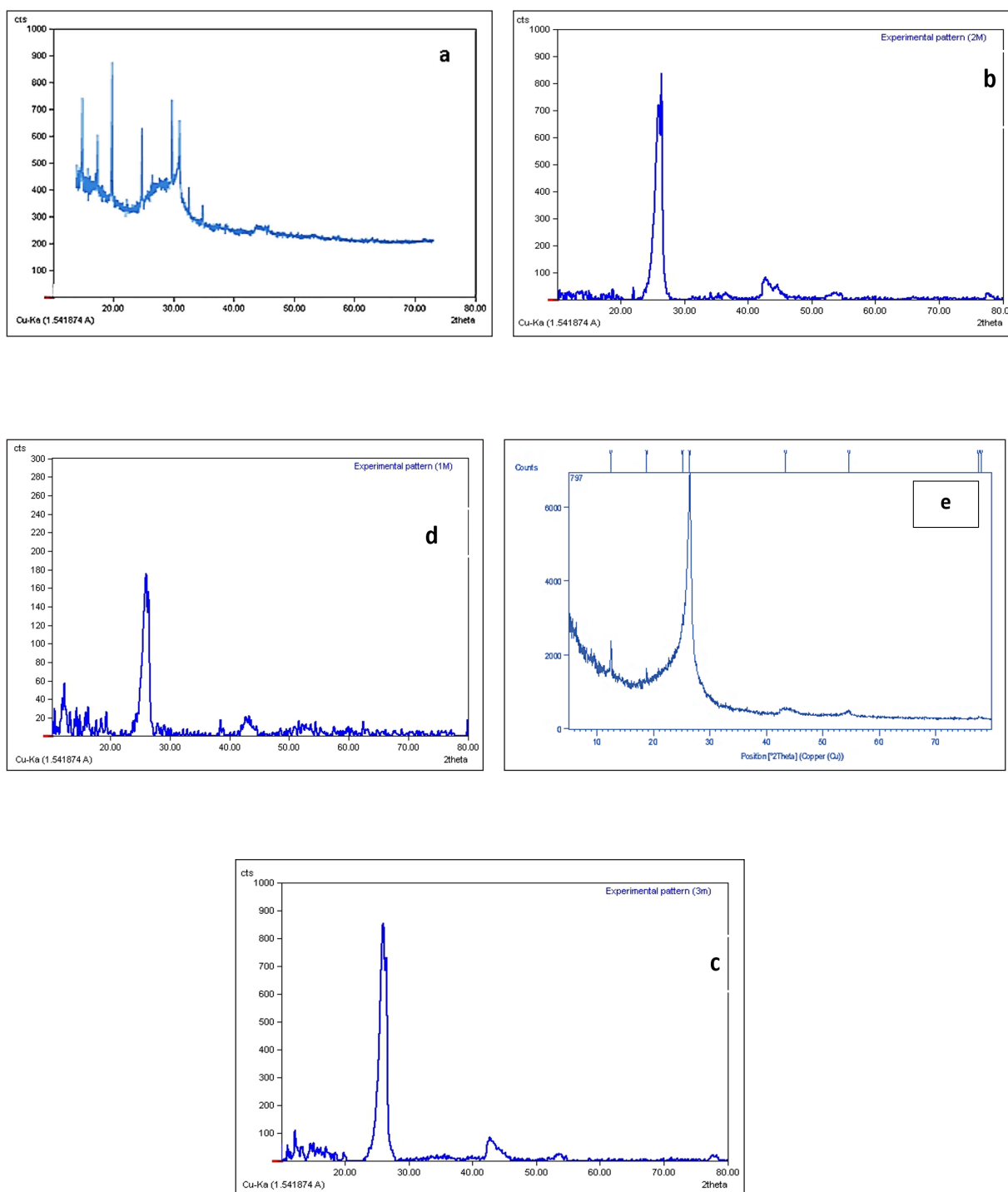


Fig. 4. XRD pattern (a) MWCNT-COOH, (b) MWCNT-Tris, (c) MWCNT-H, (d) MWCNT-Tera and (e) MWCNT-G



Fig. 5a. FE-SEM MWCNT-Tris

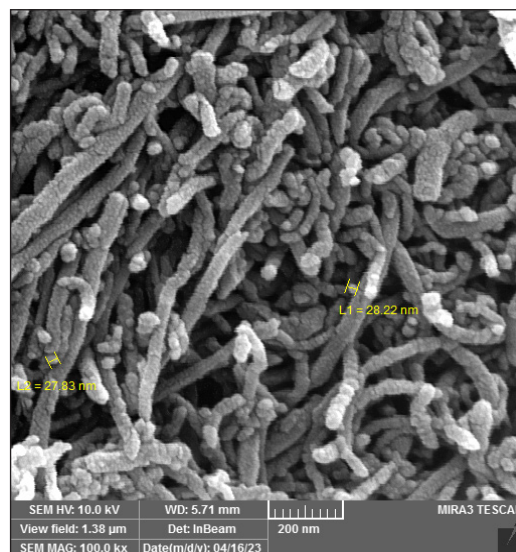


Fig. 5b. FE-SEM MWCNT-H

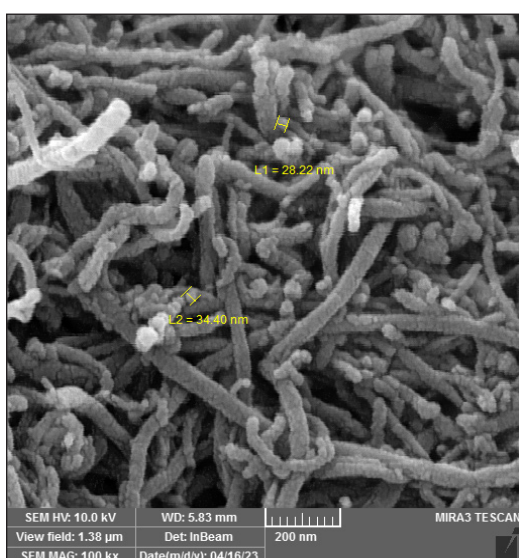


Fig. 5c. FE-SEM MWCNT-Tetra

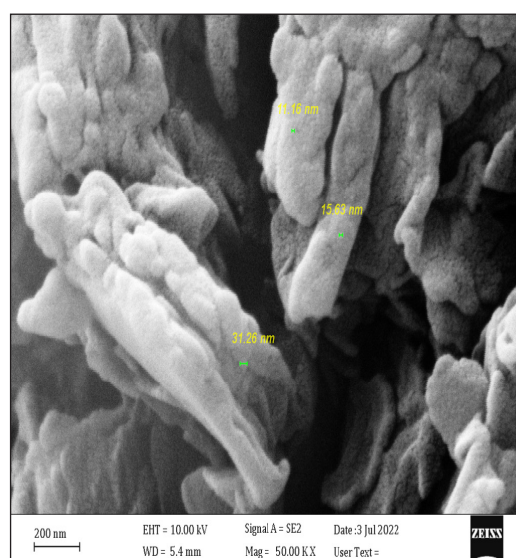


Fig. 5d. FE-SEM of MWCNT-G

Table 1. FT-IR peaks in (cm^{-1}) of MWCNTs and their Derivatives

| Groups | MWCNTs | MWCNTs-tris | MWCNTs-H | MWCNTs-tera | MWCNTs-G |
|------------------|-----------|-------------|-----------|-------------|-----------|
| -OH | 3534 | 3630 | ---- | ---- | ---- |
| -NH | ---- | 3198-3140 | 3429-3244 | 3591-3445 | 3491-3419 |
| -CH ₂ | 2940-2847 | 2904-2862 | 2940-2847 | 2940-2847 | 2940-2847 |
| C=C | 1571 | 1550 | 1593 | 1590 | 1516 |
| C=O | 1672 | 1710 | 1759 | 1793 | 1743 |
| C-N | ---- | 1109 | 1128 | 1392 | 1645 |

Table 2. Zeta Potential for MWCNTs and their Derivatives

| Potential | MWCNT | MWCNT-tris | MWCNT-H | MWCNT-tera | MWCNT-G |
|-----------|-------|------------|---------|------------|---------|
| Zeta | -36mV | -123.2mV | -46mV | -48mV | -36mV |

3. Results and Discussion

3.1. Optimization of the extraction procedure

The study for identifying the most optimal conditions for a given analytical technique involves manipulating one condition of the experiment while keeping the other factors constant. Consequently, to determine the optimal values for all components and identify the perfect conditions for achieving maximum efficiency in the process of extraction and removal of the dye [31]. The several types of investigations were executed as follows:

3.1.1. Amount of solid phase

The quantity weight of MWCNT, MWCNT/G, MWCNT/Tris, MWCNT/Tetra, or MWCNT/H was examined in this study as solid phase extraction in separation column with different range between 5-50 mg. Meanwhile, the other conditions must be fixed, as mentioned in the general method. Figure 6 shows that increasing the weight of the solid phase augments the retrieval percentage, where the recovery percentage achieves the highest value while employing a weight of 0.01g. Subsequently, the recovery percentages reached a state of stability in the biggest weights, then descending to a minimum of 0.5 g, and this observed behavior was consistent throughout all solid phases during the investigation of the BB-y dye. Consequently, a

constant weight of 0.01 g for the solid phase was chosen as the standard weight for all phases in the following tests.

3.1.2. Effect of Dye concentration

The effect of the concentrations of BB-Y dye solution has been studied after passing different concentrations (50-700) mg L⁻¹ from the day on 0.01 g of prepared solid phase, which is either one of MWCNT, MWCNT/G, MWCNT/Tris, MWCNT/Tetra, or MWCNT/H. It is essential to point out that all other experimental parameters, such as pH, dye volume, flow rate, the type and volume of elution solution, were maintained constant, as mentioned in the general procedure, where the perfect concentrations of a dye solution were 200 mg L⁻¹ and 300 mg L⁻¹ for both MWCNT and MWCNT-Tris, whereas 400 mg L⁻¹ for each of MWCNT-H, MWCNT-Terta and MWCNT-G respectively. The recovery percentage of all solid phases of MWCNTCOOH, MWCNT-Tris, MWCNT-H, MWCNT-Tetra, and MWCNT-G was obtained 60%, 63%, 62%, 66%, and 72%, respectively for the dye under the study. The proper utilization of this ratio has significance because the recovery efficiency wasn't at its highest point during this stage, and it is anticipated that it will increase by improving other conditions. Figure 7 demonstrates the effect of concentrations of BB-Y dye solution by proposed procedure.

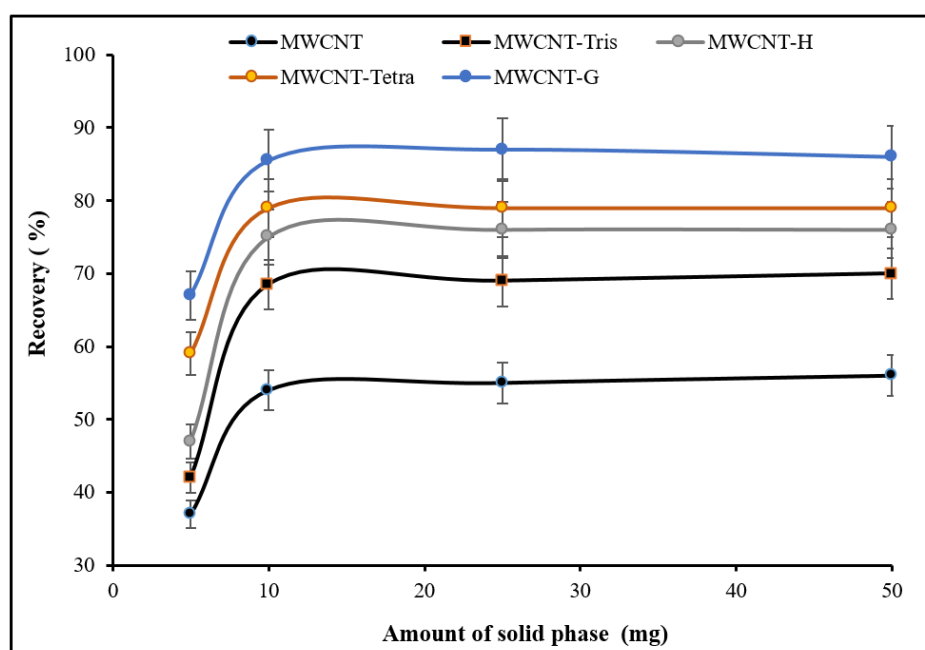


Fig. 6. Effect of the solid phase amount on the recovery of Bismarck Brown-y

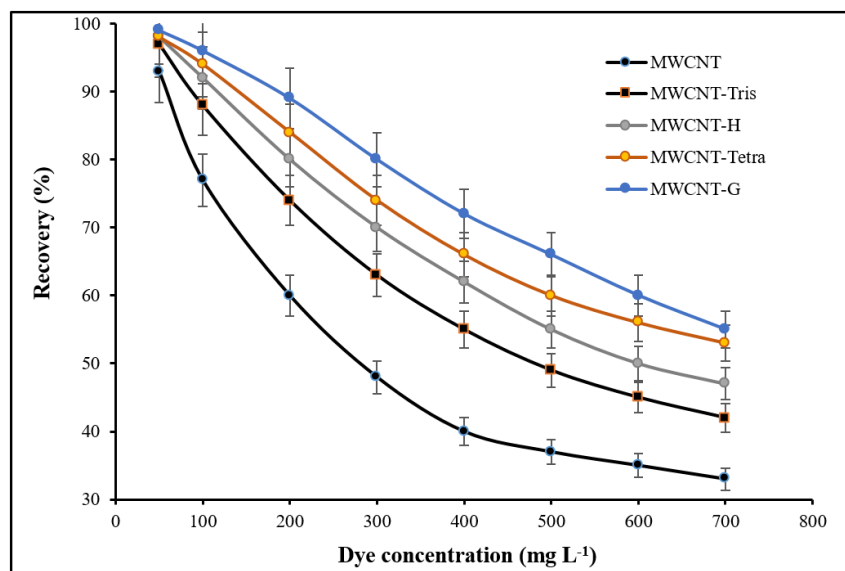
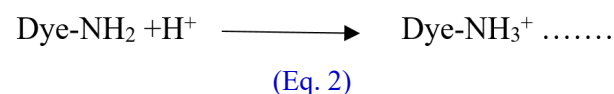


Fig. 7. Effect of Bismarck Brown-Y concentration on the recovery percentage

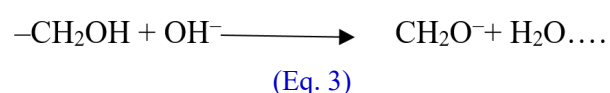
3.1.3. Effect of pH

The pH function is an essential factor in the assessment of extraction processes since it has a direct effect on the surface charge of the solid phase and the chemical structure of the dye. The effect of pH on solid phase extraction (SPE) was studied in this investigation from range 2 to 12. Figure 8 revealed that increases the recovery percentage of cationic dye (BB-Y) at pH=6 in MWCNT-Tris, whereas it was 10 for MWCNT, MWCNT-H, MWCNT-Terta, and MWCNT-G, respectively. The surface of multi-walled carbon nanotubes (MWCNTs) has a positive charge when the pH value is lower than 6.7. However, it becomes a negative charge when the pH exceeds 6.7. Therefore, the recovery ratio increases at pH 10 because of the electrostatic attraction, which accrues between the negative charges of the surface (MWCNTs) and the positive ions of dye BB-Y. On the other hand, the surface of MWCNTs in acid pH becomes the positive charge. The BB-Y converted to positive ions as a result of the protonation process, which leads to a decrease in the percentage of recovery and adsorption capacity because of electrostatic repulsion between the positive charge of the surface with the positive charge of the protonation dye [32]. As for the MWCNTs-Tris, which has three hydroxyl groups at pH 6, becomes a negative charge as zeta potential (-36 mV). Moreover, the protonation of dye leads to a charge in the nitrogen atom by the positive charge; all these reasons are due to an

increase in the adsorption capacity and recovery ratio at pH 6 (Eq. 2) [32].



However, if the pH is over 6, the dye solution becomes base, which leads to de-protonation of the nitrogen atom, and the MWCNT-tris converted more negatively as Equation 3.



Consequently, the recovery percentage and adsorption capacity decrease at a pH of more than 6 [33]. The recovery percentages for the three surfaces, MWCN-tetra, MWCN-H, and MWCN-G, are increasing at pH 10, which may be at higher pH levels. The functional groups present on the surface of the three surfaces above, such as N-H and C-H groups, can work as activation agents through negative charges. Consequently, it increased the quantity of negatively charged molecules. Therefore, the adsorption of BB-Y dye can potentially be ascribed to the significant electrostatic attraction between the charge on the three surfaces and the positively charged BB-Y molecules [34]

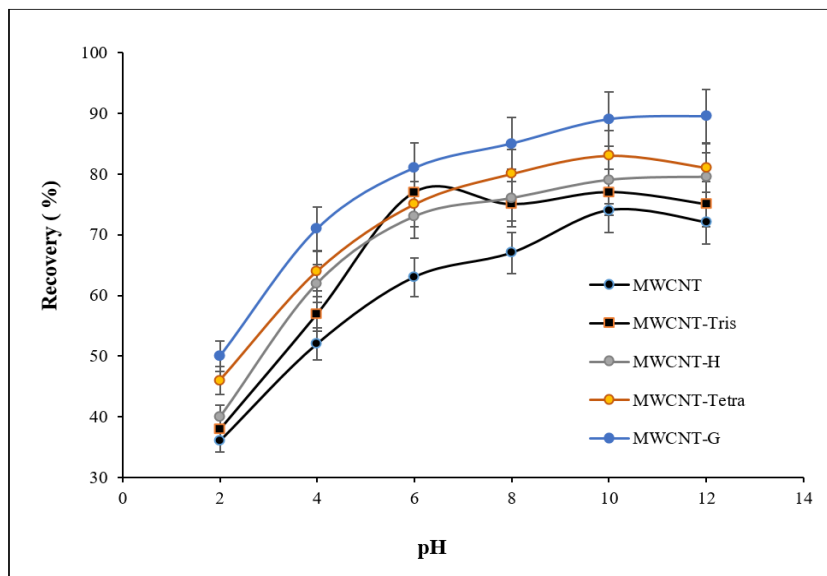


Fig. 8. Effect of pH on the recovery of Bismarck Brown-Y

3.1.4. Effect of dye volume

Investigating the impact of the volume of the solution, including the target material, is crucial in selecting the most favorable conditions for the solid-phase extraction approach [35][36]. Figure 9 illustrates the behavior of cationic dye BB-Y on five prepared surfaces, which were ordered at 74, 77, 79, 84, and 86 recoveries (%) for MWCNTCOOH, MWCNT-Tris, MWCNT-H, MWCNT-Tetra, and MWCNT-G, respectively. This study examined the different volumes of dye 1mL, 5 mL, 10 mL, 25 mL, 50 mL, and 75 mL at optimal conditions that have been obtained in previous experiments with 200mg L⁻¹ and 300mg

L⁻¹ for MWCNT and MWCNT-Tris as well as 400mg L⁻¹ for MWCNT-H, MWCNT-Tetra, and MWCNT-H, respectively. Besides, the remaining other conditions are without change as the general method. The Percentage of recovery showed a progressive reduction. The observed pattern can be attributed to a logical relationship between the extraction effectiveness and the solution's volume. Specifically, as the volume of the solution increases, the dye concentration falls, resulting in a decrease in extraction efficiency. On this fundamental, the dye will dilute with increasing the volume of the solution. Therefore, the optimal volume is 25mL for the cationic dye Bismarck brown -y.

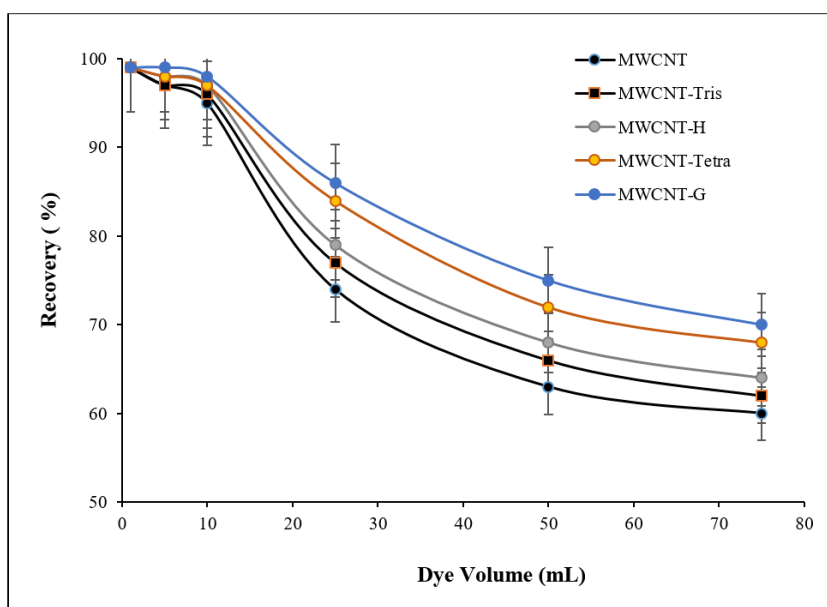


Fig. 9. Effect of Bismarck Brown-Y solution volume on the recovery percentage

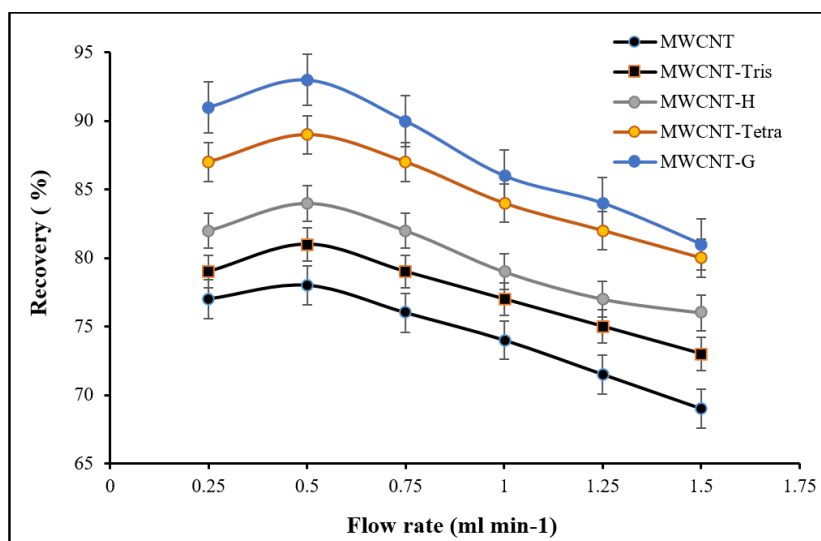


Fig.10. Effect of flow rate on the recovery of Bismarck Brown-Y

3.1.5. Effect of flow rate

One of the most important parameters influencing the efficiency of solid phase extraction is the flow rate of the dye solution. Therefore, achieving a balance in the flow rate is crucial since low flow rates hinder the attainment of high rates of recovery for the target material. This limitation arises from the potential disengagement between the solid phase and the target material. Hence, the effect of flow rate on the percentage of recovery is influenced by the connected time between the dye from one side and the solid phase on the other. The recovery percentage decreases with increasing the flow rate of the dye solution, as demonstrated in Figure 10, where 0.5 ml min⁻¹ is the perfect flow rate time for the BB-Y solution.

3.1.6. Effect of type and volume of eluting solution

The impact of different types of solvents as eluent solvents was investigated in this paper, where these solvents were chosen depending on their polarities. The polarity coefficient reveals the solvent's capacity to interact with the solute [37]. Table 3 illustrates the polarity of eluent solvents in this study. Figure 11 shows the different values of the percentage of recovery and which ordered 93, 95, 96, 98, and 99 for five surfaces under the study: MWCNTCOOH,

MWCNT-Tris, MWCNT-H, MWCNT-Tetra, and MWCNT-G, respectively. Additionally, the investigation revealed a clear correlation between the polarity of the eluent solution and the percentage of the recovery, which means that increasing the polarity of the eluent solvent increases the recovery percentage. Consequently, DMSO recorded the highest percentage since the polarity coefficient is highest at about 7.2. In contrast, other eluent solvents decrease the percentage recovery by decreasing the polarity coefficient, as obvious in Table 3. The strong affinity of BB-Y dyes towards the DMSO solvent can be ascribed to the polar nature of the dye. The dye undergoes a phase transition, then transitions from a liquid to a solid state, and subsequently migrates with the rinse solution that possesses a higher polarity (see Figure 11). Moreover, the volume of elution solvent was investigated in this study where the 5 mL of DMSO represented the perfect volume for disengagement of the cationic dye from the solid phase, as revealed in Figure 12, which illustrated the relationship between the optimal volume of elution solvent and the percentage recovery. Besides, the optimal volume of elution solvent can be calculated, by enrichment factor by Equation 4 [38].

$$\text{Enrichment Factor (EF)} = \frac{\text{Original dye volume}}{\text{Elution volume}} \quad (\text{Eq.4})$$

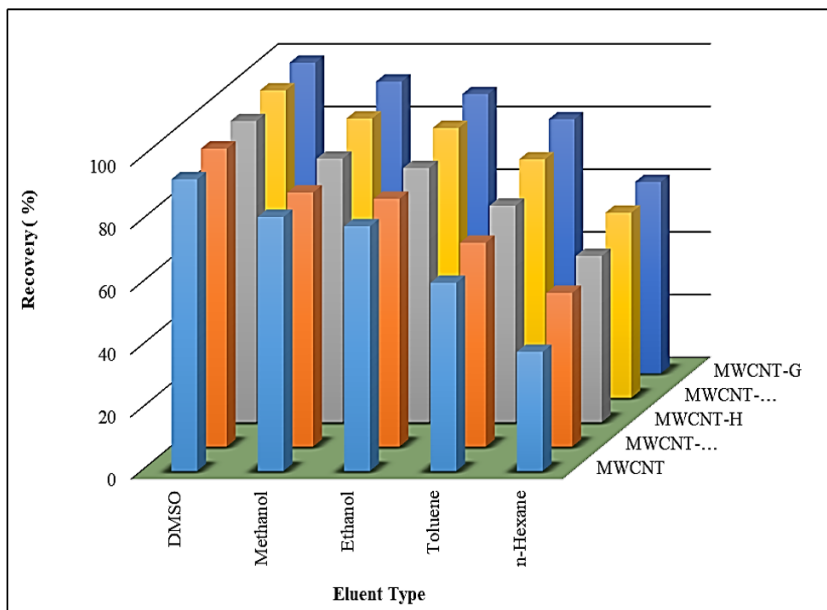


Fig 11. Effect of elution type on the recovery of Bismarck Brown-Y

Table 3. Polarity of Different Eluents that used in this study

| Solvent | Polarity Index |
|----------|----------------|
| DMSO | 7.2 |
| Methanol | 5.1 |
| Ethanol | 4.3 |
| Toluene | 2.4 |
| n-hexane | 0.1 |

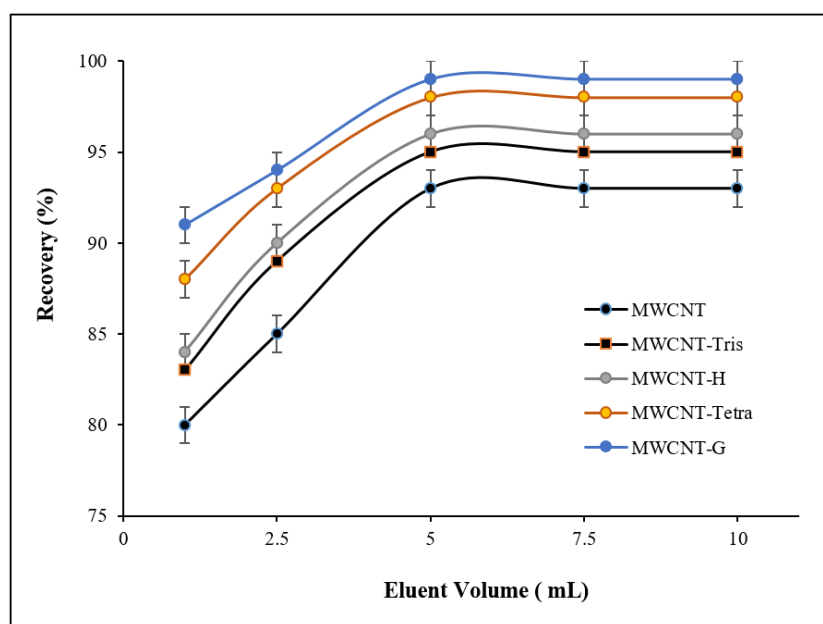


Fig 12. Effect of DMSO volume on the recovery of Bismarck Brown-Y

3.2. Isotherm study

The SPE techniques are regarded as better than other procedures due to their ease of use, flexibility to remove unwanted matrix ingredients, and capacity to attain high enrichment factors [39]. The adsorption isotherm experiments were conducted using BB-Y solutions of specific concentrations under the indicated optimal experimental conditions. By analyzing the isotherm, it becomes feasible to elucidate the correlation between the solid phases and dye and propose the underlying mechanisms of interaction [40]. Two models were used in this study to explain the adsorption isothermal compartment, which is the Langmuir model and the Freundlich model.

3.2.1. Langmuir isotherm model

The Langmuir model is reliant upon maximum adsorption, which corresponds to the emergence of a saturated monolayer of adsorbate (liquid molecules) on the adsorbent (solid surface). Equation 5 presupposes the presence of homogenous adsorption sites.

$$C_e/q_e = 1/q_{\max} K_L + 1/q_{\max}$$

(Eq.5)

Figure 13 illustrates the Langmuir model for BB-Y, where the $(1/q_{\max})$ refers to a straight line. However, the cutoff pointed out $(1/q_{\max} \times K_L)$. Consequently, the maximum adsorption capacity (q_{\max}), Langmuir constant (K_L), and correlation coefficient (R^2) were determined by the graphical representation of the Langmuir equation. This involved charting the relationship between C_e/q_e on the Y-axis and C_e on the X-axis, as mentioned in Table 4. The outcomes of the maximum adsorption capacity of BB-Y dye by solid phase (MWCNT-G) is the highest value of the others.

3.2.2. Freundlich isotherm model

The equation elucidates the phenomena of adsorption and interference occurring on heterogeneous surfaces, if adsorption occurs at active sites that have varying

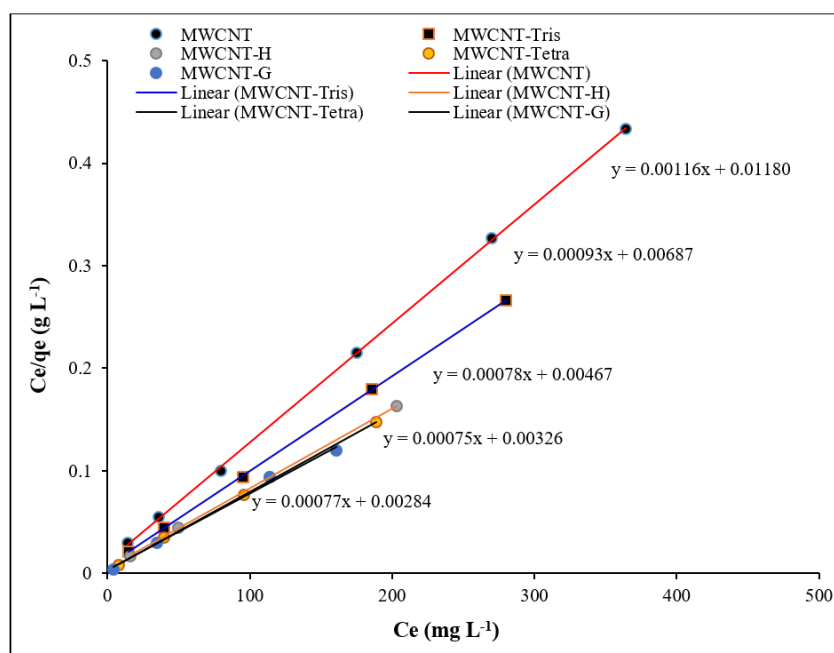


Fig. 13. Langmuir isotherm of adsorption of Bismarck Brown-y

Table 4. Langmuir isotherm parameters for the adsorption of CR dye

| Solid Phase | q_{\max} (mg g ⁻¹) | K_L | R^2 |
|-------------|----------------------------------|-------|--------|
| MWCNT | 862.068 | 0.098 | 0.9997 |
| MWCNT-Tris | 1075.268 | 0.136 | 0.9999 |
| MWCNT-H | 1282.051 | 0.169 | 0.9999 |
| MWCNT-T | 1298.701 | 0.275 | 0.9997 |
| MWCNT-G | 1333.333 | 0.234 | 0.9941 |

adsorption energies. The Freundlich equation is a mathematical model used to describe the absorption of solutes onto solid surfaces (Eq.6).

$$\ln q_e = \ln K_F + 1/n \times \ln C_e \tag{Eq.6}$$

By graphing the Freundlich equation between $\ln q_e$ on the Y-axis and $\ln C_e$ on the X-axis as in the illustration in Figure 14, the values of the Freundlich constant K_F and correlation coefficient R^2 were determined as elucidated in Table 5, where the slop of straight line refer to $1/n$. However, the cutoff refers to $\ln K_F$. The value of K_F is highest in MWCNT-G, which refers to the adsorption energy between the prepared solid phase and BB-y [30]. As a result, this outcome is compatible with the q_{max} value derived from the Langmuir equation.

The values of $1/n$ provide information about the preference or unfavorable of the adsorption process. A value of $1/n = 0$ implies irreversible adsorption, while a value between 0 and 1 indicates preferable adsorption between the solid phase and target material. On the other hand, when $1/n > 1$, adsorption may not be favorable. As observed in Table 5 the values of $1/n$ for all prepared solid phases are more than zero and less than one, which indicates the adsorption of all surfaces is preference. According to the values R^2 which had been obtained from Tables 5 and 4, Langmuir model is higher than the Freundlich model. Therefore, adsorption is a chemisorption mechanism.

4. Conclusion

The optimized method for extraction processes was conducted in this study, where the amount of solid-

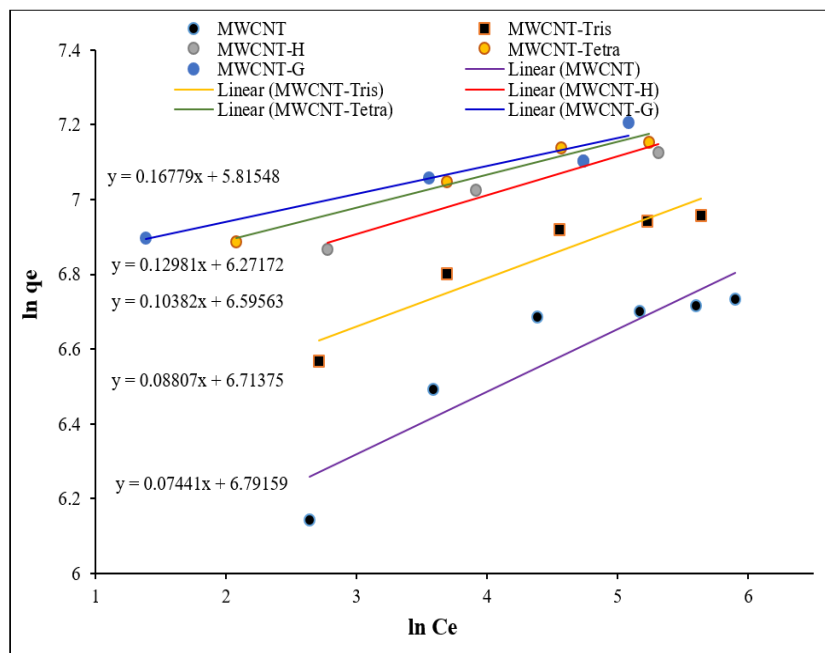


Fig. 14. Freundlich isotherm of adsorption of Bismarck Brown-y

Table 5. Freundlich isotherm parameters for the adsorption of BB-y at 25 °C

| Solid Phase | K_F | $1/n$ | R^2 |
|-------------|-------------|---------|---------|
| MWCNT | 335.452377 | 0.16779 | 0.8345 |
| MWCNT-Tris | 529.3871411 | 0.12981 | 0.89398 |
| MWCNT-H | 731.8898321 | 0.10382 | 0.96162 |
| MWCNT-Tetra | 823.6535562 | 0.08807 | 0.97272 |
| MWCNT-G | 890.3280586 | 0.07441 | 0.9385 |

phase extraction was 0.01g for all surfaces. However, the optimal concentration for Bismarck brown-y was 200 mg L⁻¹ of MWCNT and MWCN- tris while the optimal concentration was 400 mg L⁻¹ for each prepared solid phase MWCNT-H, MWCNT-tetra, and MWCNT-G. The perfect pH was 6 for MWCN-tris, and for the rest surfaces the pH was 10. The volume of dye was studied which was 25 mL. In addition, the flow rate was 0.5 ml min⁻¹ in perfect condition. Furthermore, the type of eluent solution and the optimal volume were DMSO and 5ml from it. Finally, the q_{max} was obtained at 862.0691, 1075.2689, 1282.0513, 1298.7013, and 1333.33 for the MWCNT, MWCNT-tris, MWCNT-H, MWCN-Tetra, and MWCNT-G, respectively.

5. References

- [1] A. Balasubramanian, P. A. Balasubramanian, The world's water geochemical modelling of groundwater for prevention of incrustation in the water supply systems of salem district, Tamil Nadu, Indian, View project educational video documentaries in earth, atmospheric and ocean sciences view project, 2017. <https://www.researchgate.net/publication/315123891>
- [2] P. Senthil Kumar, A critical review on recent developments in the low-cost adsorption of dyes from wastewater, *Desalin. Water Treat.*, 172 (2019) 395–416. <https://doi.org/10.5004/dwt.2019.24613>
- [3] J. C. G. Sousa, A. R. Ribeiro, M. O. Barbosa, M. F. R. Pereira, A. M. T. Silva, A review on environmental monitoring of water organic pollutants identified by EU guidelines, *J. Hazard. Mater.*, 344 (2018) 146–162. <https://doi.org/10.1016/j.jhazmat.2017.09.058>
- [4] F. F. A. Aziz, A. A. Jalil, S. Triwahyono, M. Mohamed, Controllable structure of fibrous SiO₂-ZSM₅ support decorated with TiO₂ catalysts for enhanced photodegradation of paracetamol, *Appl. Surf. Sci.*, 455 (2018) 84–95. <https://doi.org/10.1016/j.apsusc.2018.05.183>
- [5] A. Kumar Samanta, P. Agarwal, Application of natural dyes on textiles, India. *J. Fibre Textile Res.*, 34 (2009) 384-399. [https://nopr.niscpr.res.in/bitstream/123456789/6886/1/IJFTR%2034\(4\)%20384-399.pdf](https://nopr.niscpr.res.in/bitstream/123456789/6886/1/IJFTR%2034(4)%20384-399.pdf)
- [6] F. Mcyotto, Q. Wei, D. K. Macharia, M. Huang, C. Shen, C. W. K. Chow, Effect of dye structure on color removal efficiency by coagulation, *Chem. Eng. J.*, 405 (2021) 126674. <https://doi.org/10.1016/j.cej.2020.126674>
- [7] Q. Wei, F. O. Mcyotto, C. W. K. Chow, Z. Nadeem, Z. Li, J. Liu, Eco-friendly decolorization of cationic dyes by coagulation using natural coagulant Bentonite and biodegradable flocculant sodium Alginate, *SDRP J. Earth Sci. Environ. Stud.*, 5 (2020) 51–60. <https://doi.org/10.25177/jeses.5.2.ra.10648>
- [8] P. Arulmathi, C. Jeyaprabha, P. Sivasankar, V. Rajkumar, Treatment of textile wastewater by coagulation–flocculation process using gossypium herbaceum and polyaniline coagulants, *Clean Soil, Air, Water*, 47 (2019) 1800464. <https://doi.org/10.1002/clen.201800464>
- [9] N. Tara, S. I. Siddiqui, G. Rathi, S. A. Chaudhry, Inamuddin, A. M. Asiri, Nano-engineered adsorbent for the removal of dyes from water: A review, *Curr. Anal. Chem.*, 16 (2019) 14–40. <https://doi.org/10.2174/1573411015666190117124344>
- [10] S. P. Keerthana, R. Yuvakkumar, P. S. Kumar, G. Ravi, D. V. N. Vo, D. Velauthapillai, Influence of tin (Sn) doping on Co₃O₄ for enhanced photocatalytic dye degradation, *Chemosphere*, 277 (2021) 130325. <https://doi.org/10.1016/j.chemosphere.2021.130325>
- [11] S. Varjani, P. Rakholiya, H. Y. Ng, S. You, J. A. Teixeira, Microbial degradation of dyes: An overview, *Bioresour. Technol.*, 314 (2020) 123728. <https://doi.org/10.1016/j.biortech.2020.123728>
- [12] G. Crini, Non-conventional low-cost adsorbents for dye removal: A review, *Bioresour. Technol.*, 97 (2006) 1061–1085. <https://doi.org/10.1016/j.biortech.2005.05.001>
- [13] V. K. Gupta, Suhas, Application of low-cost adsorbents for dye removal-A review, *J. Environ. Manage.*, 90 (2009) 2313–2342. <https://doi.org/10.1016/j.jenvman.2008.11.017>
- [14] S. M. Ghoreishi, R. Haghghi, Chemical catalytic reaction and biological oxidation for treatment of non-biodegradable textile effluent, *Chem. Eng. J.*, 95 (2003) 163–169. [https://doi.org/10.1016/S1385-8947\(03\)00100-1](https://doi.org/10.1016/S1385-8947(03)00100-1)
- [15] M. Rezaei, A. Habibi-Yangjeh, Simple and large scale refluxing method for preparation of Ce-doped ZnO nanostructures as highly efficient photocatalyst, *Appl. Surf. Sci.*, 265 (2013) 591–596. <https://doi.org/10.1016/j.apsusc.2012.11.053>
- [16] B. Mu, A. Wang, Adsorption of dyes onto palygorskite and its composites: A review, *J. Environ. Chem. Eng.*, 4 (2016) 1274–1294. <https://doi.org/10.1016/j.jece.2016.01.036>
- [17] X. Hou, S. Tang, J. Wang, J. Wang, Recent

- advances and applications of graphene-based extraction, *Trends Anal. Chem.*, 119 (2019) 115603. <https://doi.org/10.1016/j.trac.2019.07.014>
- [18] E. Dziurkowska, M. Wesolowski, Solid phase extraction purification of saliva samples for antipsychotic drug quantitation, *Molecules.*, 23 (2018) 2946. <https://doi.org/10.3390/molecules23112946>
- [19] Y. Wen, L. Chen, J. Li, D. Liu, L. Chen, Recent advances in solid-phase sorbents for sample preparation prior to chromatographic analysis, *TrAC Trends Anal. Chem.*, 59 (2014) 26–41. <https://doi.org/10.1016/j.trac.2014.03.011>
- [20] S. Di, Recent advances and applications of magnetic nanomaterials in environmental sample analysis, *TrAC Trends Anal. Chem.*, 126 (2020) 115864. <https://doi.org/10.1016/j.trac.2020.115864>
- [21] C. Jamshidzadeh, A new analytical method based on bismuth oxide-fullerene nanoparticles and photocatalytic oxidation technique for toluene removal from workplace air, *Anal. Methods Environ. Chem. J.* 2 (2019) 73-86. <https://doi.org/10.24200/amecj.v2.i01.55>
- [22] M Arjomandi, A review: analytical methods for heavy metals determination in environment and human samples, *Anal. Methods Environ. Chem. J.*, 2 (2019) 97-126. <https://doi.org/10.24200/amecj.v2.i03.73>
- [23] R. Ashouri, Dynamic and static removal of benzene from air based on task-specific ionic liquid coated on MWCNTs by sorbent tube-headspace solid-phase extraction procedure, *Int. J. Environ. Sci. Technol.*, 18 (2021) 2377-2390. <https://doi.org/10.1007/s13762-020-02995-4>
- [24] J. Rakhtshah, A rapid extraction of toxic styrene from water and wastewater samples based on hydroxyethyl methylimidazolium tetrafluoroborate immobilized on MWCNTs by ultra-assisted dispersive cyclic conjugation-micro-solid phase extraction, *Microchem. J.*, 170 (2021) 106759. <https://doi.org/10.1016/j.microc.2021.106759>
- [25] S. Teimoori, An immobilization of aminopropyl trimethoxysilane-phenanthrene carbaldehyde on graphene oxide for toluene extraction and separation in water samples, *Chemosphere*, 316 (2023) 137800. <https://doi.org/10.1016/j.chemosphere.2023.137800>
- [26] S. Teimoori, A.H. Hassani, M. Panahi, N. Mansouri, Rapid extraction of BTEX in water and milk samples based on functionalized multi-walled carbon nanotubes by dispersive homogenized-micro-solid phase extraction, *Food Chem.*, 421 (2023) 136229. <https://doi.org/10.1016/j.foodchem.2023.136229>
- [27] S. Teimoori, A.H. Hassani, New extraction of toluene from water samples based on nano-carbon structure before determination by gas chromatography, *Int. J. Environ. Sci. Technol.*, 20 (2023) 6589–6608. <https://doi.org/10.1007/s13762-023-04906-9>
- [28] B. Ali, Preparation of carbon nanotubes via chemical technique (modified staudenmaier method), *Nanosci. Nanotechnol. Asia*, 7 (2017) 113–122. <https://doi.org/10.2174/2210681206666160711161421>
- [29] Z. B. Ali Abdalnabi, H. T. Abdulsahib Faris, A J Al-doghachi, Synthesis and characterization of some selenazone complexes and nanoadsorbent surfaces from industrial waste for removing some carcinogenic dyes and heavy metals from water, proposal, 2021. <https://faculty.uobasrah.edu.iq/uploads/publications/1643354925.pdf>.
- [30] M. H. Abdel-Aziz, DFT and experimental study on adsorption of dyes on activated carbon prepared from apple leaves, *Carbon Lett.*, 31 (2021) 863–878. <https://doi.org/10.1007/s42823-020-00187-1>
- [31] T. N. Majid, A. A. Abdulwahid, An efficient cheap source of activated carbon as solid phases for extraction and removal of Congo Red from aqueous solutions, *Anal. Methods Environ. Chem. J.*, 5 (2022) 40–54. <https://doi.org/10.24200/amecj.v5.i03.205>
- [32] M. I. Mohammed, S. Baytak, Synthesis of bentonite–carbon nanotube nanocomposite and its adsorption of rhodamine dye From water, *Arab. J. Sci. Eng.*, 41 (2016) 4775–4785. <https://doi.org/10.1007/s13369-016-2190-7>
- [33] G. Z. Kyzas, N. K. Lazaridis, Reactive and basic dyes removal by sorption onto chitosan derivatives, *J. Colloid Interface Sci.*, 331 (2009) 32–39. <https://doi.org/10.1016/j.jcis.2008.11.003>
- [34] G.Z. Kyzas, D.N. Bikiaris, N. K. Lazaridis, Low-swelling chitosan derivatives as biosorbents for basic dyes, *Langmuir.*, 24 (2008) 4791–4799. <https://doi.org/10.1021/la7039064>
- [35] A. A. Gouda, W. A. Zordok, Solid-phase extraction method for preconcentration of cadmium and lead in environmental samples using multiwalled carbon nanotubes, *Turk. J. Chem.*, 42 (2018) 1018–1031. <https://doi.org/10.3906/kim-1711-90>

- [36] M. Hossein, N. Dalali, A. Karimi, K. Dastanra, Solid phase extraction of copper, nickel, and cobalt in water samples after extraction using surfactant coated alumina modified with indane-1, 2, 3-trione 1, 2-dioxime and determination by flame atomic absorption spectrometry, *Turk. J. Chem.*, 34 (2010) 805–814. <https://doi.org/10.3906/kim-1002-22>
- [37] L. R. Snyder, Classification off the solvent properties of common liquids, *J. Chromatogr. Sci.*, 16 (1978) 223–234. <https://doi.org/10.1093/chromsci/16.6.223>
- [38] Y. Li, W. Zhang, R. G. Wang, P. L. Wang, X. O. Su, Development of a efficient and sensitive dispersive liquid-liquid microextraction technique for extraction and preconcentration of 10 β -Agonists in animal urine, *PLOS One*, 10 (2015) e0137194. <https://doi.org/10.1371/journal.pone.0137194>
- [39] G. Daneshvar Tarigh, F. Shemirani, Simultaneous in situ derivatization and ultrasound-assisted dispersive magnetic solid phase extraction for thiamine determination by spectrofluorimetry, *Talanta.*, 123 (2014) 71–77. <https://doi.org/10.1016/j.talanta.2014.01.045>
- [40] E. Yilmaz, G. Guzel Kaya, H. Deveci, Removal of methylene blue dye from aqueous solution by semi-interpenetrating polymer network hybrid hydrogel: Optimization through Taguchi method, *J. Polymer Sci., Part A: Polymer Chem.*, 57 (2019) 1070–1078. <https://doi.org/10.1002/pola.29361>